Compressible Gas Flow

by

Elizabeth Adolph

Submitted to

Dr. C. Grant Willson

CHE253M
Department of Chemical Engineering
The University of Texas at Austin

Fall 2008

Compressible Gas Flow

Abstract

In this lab, compressible gas flow through a piping system consisting of a critical flow nozzle, pressure gauges, flow meters, orifices, and a tank was observed. The critical pressure ratio (the outlet pressure divided by the inlet pressure) for choked flow through a nozzle was determined by slowly increasing the downstream pressure and observing the point at which the mass flow rate began to change. The critical pressure ratio was calculated to be 0.704, and the minimum inlet to outlet pressure ratio for choked flow was determined to be 1.42. The manufacturer's performance curve for sonic flow was calibrated versus a National Institute of Standards and Technology (NIST) digital flow meter. The calibration equation was determined to be $y = 1.012\ x - 0.001166$, where y is the manufacturer's flow rate in lb / min and x is the NIST flow rate in lb / min. The discharge coefficients of an orifice as a function of Reynolds number were determined by measuring the flow rate and pressure drop across the orifice. The discharge coefficient was calculated to be 0.920 at a Reynolds number of 12700, 0.926 at a Reynolds number of 18500, and 0.935 at a Reynolds number of 21600. These values were about 47% larger than the literature values from Perry's Handbook. Finally, the pressure in a tank was monitored versus time as it was discharged by sonic flow through several different orifices. K', the orifice constant, was calculated from the slope of a plot of ln(P) versus time for each of four trials using orifices with known diameters. The average K' was -10.67 ± 0.31. The diameter of the unknown orifice was calculated using this experimental K' and was determined to be 0.045". For an initial pressure of 90 psig and final pressure of 30 psig, the fraction of mass of air escaped from the tank was 0.457, and the absolute amount of gas escaped was 40.7 g. The tank discharges faster through the 0.055" orifice than through the 0.03" and 0.04" orifices combined because the area of the 0.055" orifice is larger than the sum of the areas of the 0.030" and 0.040" orifices (Willson, 2008).

Contents

Compressible Gas Flow

Introduction

The purpose of this experiment was to measure properties of compressible gas flow under both sonic and subsonic conditions. First, the critical pressure ratio for a critical flow nozzle was determined. The upstream temperature and pressure were kept constant and the downstream pressure was increased until the mass flow rate began to change. The nozzle manufacturer's performance curve was calibrated against the NIST-calibrated digital flow meter by calculating the choked mass flow rates predicted by the performance curve at each value of the upstream pressure and plotting them against the NIST flow rate (Willson, 2008).

The discharge coefficients of an orifice meter were calculated at three different Reynolds numbers by determining the upstream pressure, upstream temperature, pressure drop across the orifice, and flow rate through the orifice. These experimental discharge coefficients were compared to literature values of the discharge coefficient from Perry's Handbook (Willson, 2008).

Finally, the pressure in a tank was monitored versus time as the air in the tank discharged through one or two orifices. This procedure was repeated using three orifices with known diameters and one orifice with an unknown diameter. The slopes of the plots of the natural log of pressure versus time for the known orifices were used to calculate the orifice constant K'. The calculated K' and the slope of the plot of ln(P) versus time for the unknown orifice were used to determine the unknown diameter (Willson, 2008).

Methods

The flow of air, a compressible gas, was observed in this experiment. The density of a compressible fluid changes with both position and time. The mass flow rate is constant because no accumulation occurs, so the volumetric flow rate and velocity of the fluid also change with position. Sonic flow occurs when the velocity of the fluid equals the speed of sound in the fluid. The Mach number (M) is the ratio of the fluid velocity to the speed of sound, so sonic flow occurs when M equals one. For values of M less than one, subsonic flow occurs; for values of M greater than one, supersonic flow occurs (Willson, 2008).

The apparatus consisted of a piping system with a flow meter, several pressure gauges, a differential manometer, several orifice meters, and a tank. Air was supplied through a main ball valve. A diagram of the experimental apparatus is displayed in Appendix D (Willson, 2008).

In the first part of the experiment, the critical pressure ratio for sonic flow through a critical flow nozzle was determined. The critical pressure ratio is the ratio of the downstream pressure to the upstream pressure at which the flow becomes sonic. Below the critical pressure ratio, the mass flow rate is constant for a given upstream pressure. The flow is choked, and it does not change if the downstream pressure is decreased. If the downstream pressure is increased so the pressure ratio is higher than the critical ratio, the mass flow rate will decrease, and subsonic flow will occur. In this experiment, the upstream pressure was kept constant, and the downstream pressure was slowly increased

from 0 psig. The flow rate at each downstream pressure was recorded, and a plot of mass flow rate versus pressure ratio was developed. The downstream pressure at which the flow rate first began to change was used to determine the critical pressure ratio. This procedure was repeated using four different values of upstream pressure (Willson, 2008).

NIST-calibrated digital handheld manometers were used to determine the upstream and downstream pressures. These devices are strain gauge transducers with semiconductors. The change in resistance of the semiconductor is proportional to the change in pressure. Also, a NIST-calibrated digital flow meter was used to monitor the flow rate of the gas. A percentage of the flow through the meter enters a stainless steel sensor tube. Heat is applied to the gas, causing the resistance of a heater sensor coil to change. The temperature-dependent resistance change is proportional to the mass flow rate through the meter (Willson, 2008).

The critical mass flow rate at each upstream pressure was calculated using Equation 1, where w is the mass flow rate, P is the upstream pressure, T is the upstream temperature, and K is a function of pressure for a specific gas and nozzle. The value of K was determined using the manufacturer's performance curve provided in the lab manual. The calculated mass flow rate was compared to the flow rate determined using the NIST flow meter, and a calibration plot for the performance curve was developed (Willson, 2008).

$$w_{CFN} = \frac{KP_1}{\sqrt{T_1}} \tag{1}$$

In the second part of the experiment, compressible gas flow through an orifice was studied. An orifice is an obstruction meter used to determine the flow rate of a fluid. At the orifice, the diameter decreases to a minimum, so the velocity of the fluid reaches a maximum and the pressure reaches a minimum. Bernoulli's equation (see Equation 2) describes the energy balance across the orifice, where P is pressure, ρ is density, V is velocity, g is the acceleration due to gravity, and h is the height. Since the pipe near the orifice was horizontal, the height difference term is zero (Willson, 2008).

$$P_1 + \frac{1}{2}\rho_1 V_1^{\,2} + \rho_1 g h_1 = P_2 + \frac{1}{2}\rho_2 V_2^{\,2} + \rho_2 g h_2 \tag{2}$$

Bernoulli's equation can be used to find the volumetric flow rate of the fluid. Because the air flow is compressible, an expansion factor, Y, is used to account for the change in the density of the fluid. For gases, Y is calculated using Equation 3, where r is the ratio of the downstream pressure to the upstream pressure, β is the ratio of the diameter of the orifice to the diameter of the pipe, and γ is the specific heat capacity ratio (Cp / Cv). Although some of the pressure loss through the orifice is recovered downstream of the meter, some of it is permanently lost. Therefore, the discharge coefficient Cd is used to account for the permanent pressure loss. Equation 4 is the equation used to calculate the volumetric flow rate of a compressible fluid through an orifice. Q is the volumetric flow rate, P is pressure, ρ is density, and A is the area of the orifice (Willson, 2008).

$$Y = \sqrt{r^{2/\gamma}\left(\frac{\gamma}{\gamma-1}\right)\left(\frac{1-r^{(\gamma-1)/\gamma}}{1-r}\right)\left(\frac{1-\beta^4}{1-\beta^4 r^{2/\gamma}}\right)} \quad (3)$$

$$Q = C_d A_2 Y \sqrt{\frac{2(\Delta P)}{\rho_1(1-\beta^4)}} \quad (4)$$

The flow rate, upstream temperature, upstream pressure, and pressure drop across the orifice were measured at three different Reynolds numbers. These values and the diameters of the orifice and pipe given in the lab manual were used to calculate the discharge coefficient and Reynolds number of each trial. The calculated discharge coefficients were compared to the discharge coefficients given in Perry's Handbook (Willson, 2008).

Finally, pressure in a tank was relieved through several orifice meters as the pressure was monitored versus time. The pressure in the tank was measured using a Schaevitz strain gauge transducer. The gauge converts pressure, a physical signal, to voltage, an analog signal. As pressure changes, the metal foil in the gauge deforms, and its resistance changes. The resistance change creates a small potential that is output by the gauge. The gauge was calibrated using the NIST-calibrated digital handheld manometer, and the output voltages were converted to pressure using the experimental calibration equation (Willson, 2008).

Since sonic flow occurred through the orifices at the tank pressure used in this lab, Equation 1 can be applied to determine the mass flow rate out of the tank. This equation was used to determine the relationship between pressure and time. Equation 5 describes the pressure in the tank as a function of time, where P is absolute pressure, K' is a constant for a given gas, temperature, and tank volume, d is the diameter of the orifice, and t is time (Willson, 2008).

$$\ln P = K' d^2 t + constant \quad (5)$$

K' was calculated from the slopes of the plots of ln(P) versus time for the orifices with known diameters. These values were averaged together and used to determine the diameter of the unknown orifice. The fraction of mass remaining in the tank at a given pressure was calculated using Equation 6, where P is the pressure in the tank, P0 is the initial tank pressure, f is the fraction of mass remaining, and γ is the specific heat capacity ratio. The absolute mass remaining was calculated by multiplying the fraction remaining by the initial mass in the tank (determined using the ideal gas law). The mass of gas escaped was calculated by subtracting the amount remaining in the tank from the initial mass (Willson, 2008).

$$P = P_0 f^{\gamma} \quad (6)$$

Results

The critical pressure ratio for which sonic flow occurred at the throat of the nozzle was determined by finding the first value of P2 for which the mass flow rate changed. The pressures output by the digital manometers were gauge pressures, but all equations used in this lab required absolute pressures. Therefore, all gauge pressures were converted to absolute pressures by adding the atmospheric pressure, which was 14.4 psia. In addition, the temperatures in °F were converted to absolute temperatures in °R by adding 460. The standard volumetric flow rate was converted to actual volumetric flow rate.

The mass flow rate was calculated using Equation 7. The density of air at atmospheric conditions was constant, so the mass flow rate was directly proportional to the volumetric flow rate. There was error in the last digit of the volumetric flow meter reading, so the uncertainty in the flow rate was +/- 0.1 L/min. For each inlet pressure, the point at which the flow rate changed by at least 0.2 L/min was used to find the critical ratio. These critical pressure ratios were verified by plotting the mass flow rate versus the ratio of P2 / P1 over the entire range of data collected (see Figs. 1–4). The point at which the mass flow rate changed was determined visually. The solid horizontal line illustrates the flow rate of choked flow through the nozzle, and the dashed vertical line shows the critical pressure ratio. The critical pressure ratios determined using these two methods were equal within +/- 0.005, and they were averaged together in order to determine the experimental critical pressure ratio for the nozzle.

$$w = Q_{DFM} \bullet \rho_{DFM} = \frac{Q_{DFM} P_{atm} M_{air}}{R T_{atm}} \qquad (7)$$

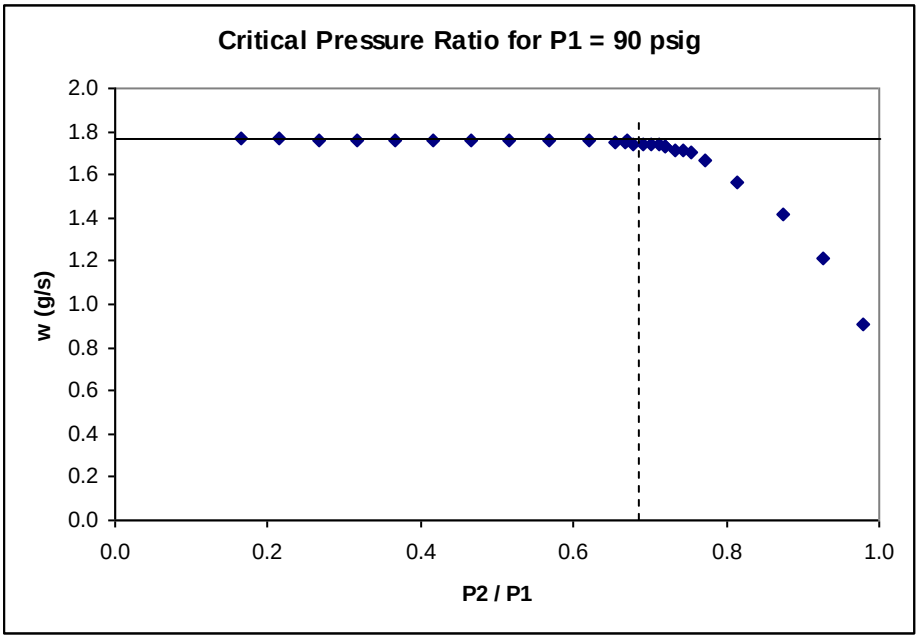

Figure 1. Visual determination of critical pressure ratio for P1 = 90 psig

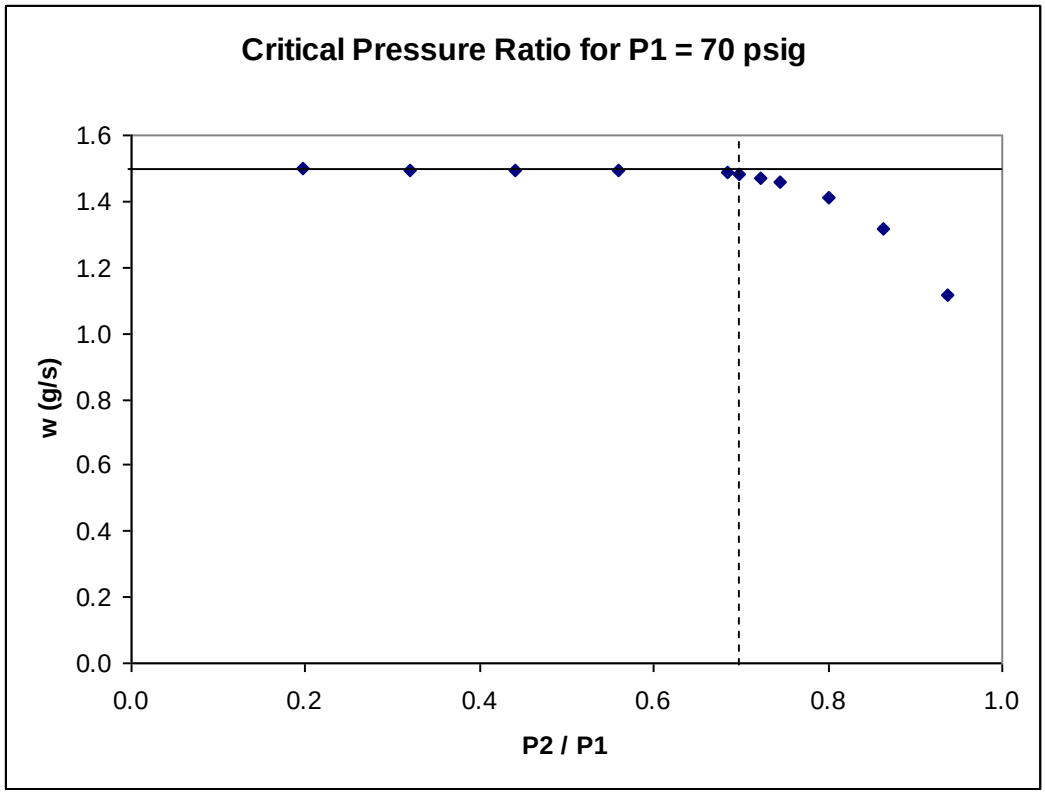

Figure 2. Visual determination of critical pressure ratio for P1 = 70 psig

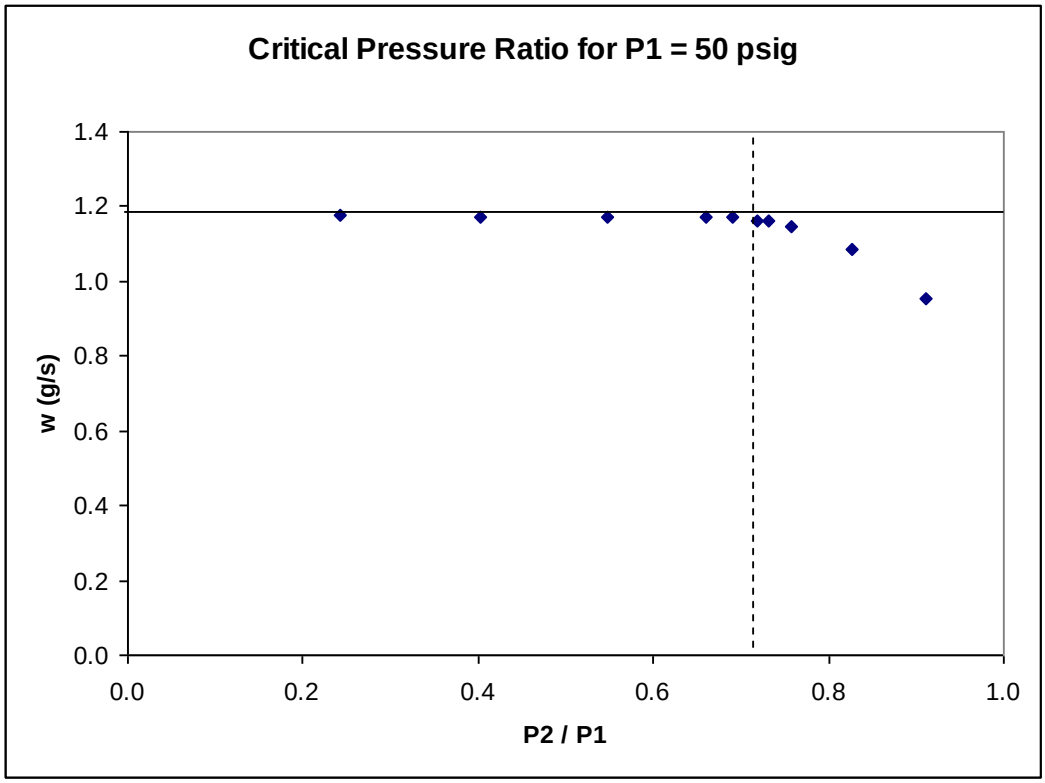

Figure 3. Visual determination of critical pressure ratio for P1 = 50 psig

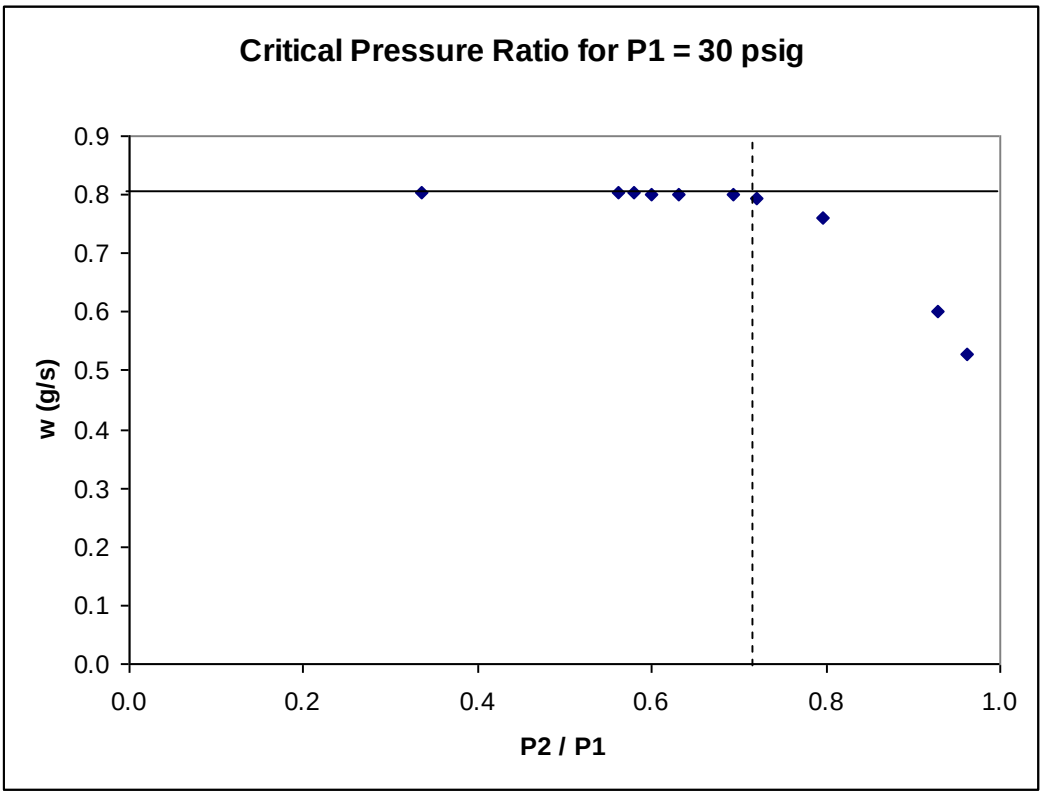

Figure 4. Visual determination of critical pressure ratio for P1 = 30 psig

Table 1 displays the values of P1, P2, and the pressure ratio at which critical flow occurred. The average critical pressure ratio was 0.704. The manufacturer claims that critical flow can be maintained at P1 / P2 ratios as low as 1.2, which means critical flow can occur at P2 / P1 ratios as high as 0.833. The experimental results contradict this claim because the calculated critical pressure ratio was 0.704, which is less than 0.833. Therefore, sonic flow can only occur at P2 / P1 ratios up to 0.704. Above that ratio, subsonic flow will occur. The experimental results suggest that the lowest inlet to exit pressure ratio at which critical flow can occur is 1.42.

Table 1. Determination of critical pressure ratio

P1 (psia)	P2 (psia)	r_c
97.9	66.3	0.677
82.4	57.5	0.698
64.8	46.5	0.718
44.5	32.1	0.721

The precision and accuracy of the flow rate obtained from the performance curve were determined by plotting the flow rate calculated using the manufacturer's performance curve versus the flow rate output of the NIST-calibrated digital flow meter. The NIST flow rate was calculated by converting the standard volumetric flow rate to the actual flow rate and multiplying by the density at atmospheric conditions (see Equation

7). The manufacturer's flow rate was calculated using Equation 8, where T1 and P1 are the upstream temperature and pressure and K is determined from the performance curve. The calibration plot and equation are shown in Fig. 5. The 95% confidence limits of the slope are 1.012 ± 0.043, and the 95 % confidence limits of the intercept are – 0.001166 ± 0.007686 lb / min. The confidence intervals of the slope and intercept are a measure of the precision of the manufacturer's flow rate. A precise flow rate will have small confidence intervals. The plot shows that the confidence limits are small, so the manufacturer's flow rate is very precise. The confidence limits become larger the farther the flow rate is from the measured range (0.10 – 0.23 lb / min). The R^2 value was 0.9998, which is very close to one, so the manufacturer's flow rate had a strong linear correlation to the true flow rate.

$$w_{CFN} = \frac{KP_1}{\sqrt{T_1}} \tag{1}$$

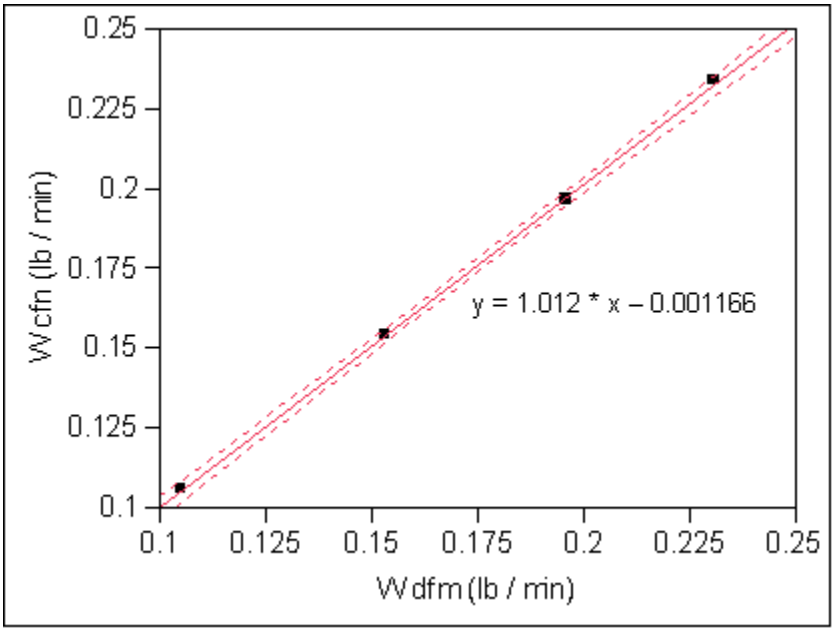

Figure 5. Calibration plot for nozzle manufacturer's performance curve

If the nozzle flow rate is perfectly accurate, it will have a slope of one and an intercept of zero. The difference between the actual slope and one is 0.012, and the difference between the actual intercept and zero is – 0.001166 lb / min. The difference between the true flow rate and the flow rate predicted by the nozzle manufacturer is a measure of the accuracy of the performance curve. Fig. 6 displays the difference between the calibration curve and the line y = x. The performance curve is most accurate near flow rates of 0.0972 lb / min. This flow rate is the point at which the manufacturer's flow rate equals the true flow rate, which is the point at which the calibration equation crosses the line y = x. The accuracy error increases the farther the flow rate is from 0.0972 lb / min. Based on the difference plot, the largest error in the accuracy of the manufacturer's flow rate in the range of flow rates examined in this lab (0.10 – 0.23 lb / min) was 0.0016 lb / min.

It would be helpful to compare the relative precision and accuracy of the manufacturer's curve with the precision and accuracy of other flow meters. The experiment could be improved by measuring the flow rate with several different flow meters and calibrating all of the meters with the NIST standard. Then the accuracy and precision of the performance curve could be compared to the accuracy and precision of various flow meters in order to determine how useful the performance curve is and in which flow rate ranges it is useful.

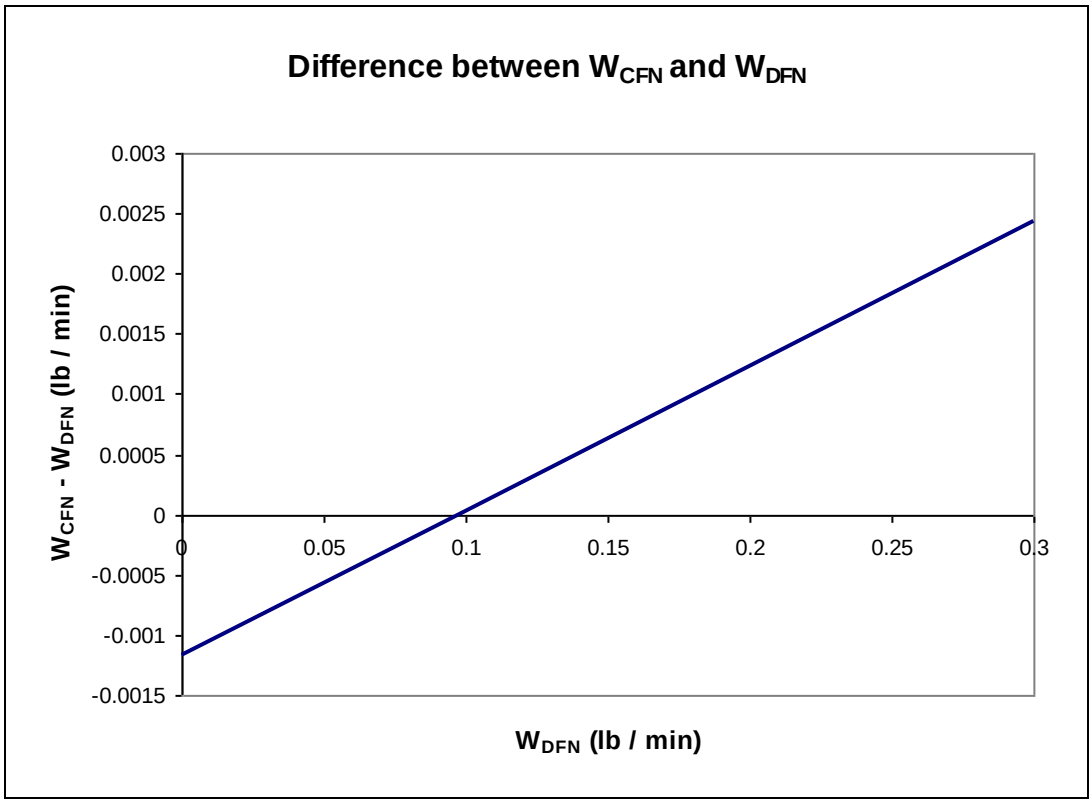

Figure 6. Difference between NIST flow rate and manufacturer's flow rate

The discharge coefficients (Cd) and Reynolds numbers (Re) of the flow through the orifice for three different pressure drops were calculated using Equations 9 and 10. The pressures (except the pressure differentials) and temperatures were converted to absolute values, and the flow rates were converted from standard to actual. Sample calculations are shown in Appendix B. The calculated discharge coefficients as well as the literature values from Perry's Handbook are displayed in Table 2.

$$C_d = \frac{Q}{A_2 Y}\sqrt{\frac{\rho_1(1-\beta^4)}{2g_c(\Delta P)}} \tag{9}$$

$$\mathrm{Re} = \frac{\rho_{atm} V_{or} d_{or}}{\mu_{air}} \tag{10}$$

Table 2. Discharge coefficients of orifice at several Reynolds numbers

ΔP (in H2O)	Re	Experimental Cd	Theoretical Cd (Green, 2008)
5.1	12700	0.920	0.63
11.0	18500	0.926	0.62
15.0	21600	0.935	0.62

The experimentally determined discharge coefficients are much larger than the theoretical values (around 47% larger). An ideal orifice with no permanent pressure loss will have a discharge coefficient of one. The actual pressure loss will always be greater than zero (unless energy is added to the system), so actual discharge coefficients are less than one. The high calculated discharge coefficients suggest that there is less permanent pressure loss than is theoretically predicted. Also, the theoretical values decrease slightly as the Reynolds number increases while the experimental values increase as the Reynolds number increases. The experiment could be improved by finding the discharge coefficient at a wider range of Reynolds numbers. By doing so, the experimental and theoretical discharge coefficients could be compared over a larger portion of the curve from Perry's Handbook.

There were large errors (around 47%) in the difference between the calculated and theoretical discharge coefficients. There were large random errors in the readings from the differential manometer because the water level in both sides of the manometer fluctuated greatly. This error resulted in large relative errors that were propagated through the calculations because the magnitude of the pressure drop was small. Also, it is possible that the orifice used in this lab was a different type than the orifice used to determine the literature values. The literature values are for square-edged orifices with corner taps, so it is possible that the experimental orifice is not square-edged or does not have corner taps. The orifice used in this lab may have been specially designed in order to improve performance and increase the discharge coefficient.

In the tank bleeddown experiment, the pressure in the tank was discharged five times through different orifices. The experiment was performed using the 0.030" orifice, the 0.040" orifice, the 0.055" orifice, the unknown orifice, and the combination of the 0.030" and 0.040" orifices. In order to determine the relationship between the pressure in the tank and time, the Schaevitz strain gauge used in this part of the experiment was calibrated against the NIST-calibrated digital handheld manometer. The calibration plot for the strain gauge output in mV versus the manometer output in psig is displayed in Fig. 7. The 95% confidence intervals are also illustrated on the plot, but they are too small to be seen.

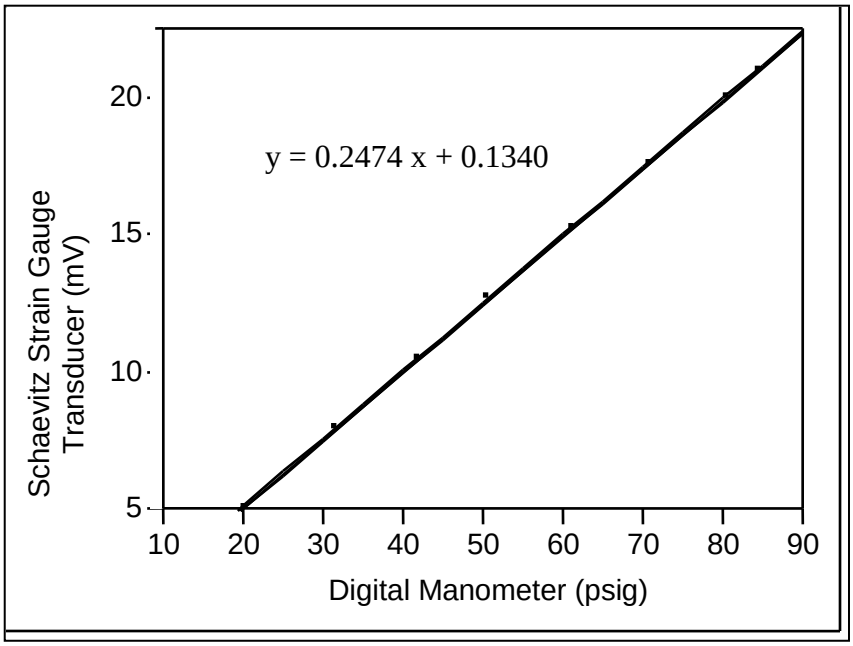

Figure 7. Calibration of the Schaevitz strain gauge

Figs. 8 – 12 show the plots of ln(P) versus time for the five trials. In the equations displayed on the graphs, y is ln(P) and x is time in seconds. Table 3 displays the confidence limits of the slope and intercept of each plot. The intercepts of the plots are meaningless since the trials were started at different times and at slightly different initial pressures. The slopes of the lines of best fit were used to calculate the value of K' (see Equation 11). K' and its 95% confidence limits were calculated to be -10.67 ± 0.31. This experimental K' and the slope of the plot of ln(P) versus time for the unknown orifice were used to calculate the unknown orifice diameter, which was determined to be 0.045". Sample calculations are shown in Appendix B.

$$slope = K' d^2 \qquad (11)$$

Table 3. Slopes, intercepts, and confidence intervals of ln(P) versus t plots

Orifice	Slope ± 95% CI	Intercept ± 95% CI
0.030"	– 0.00960 ± 0.00010	4.95 ± 0.0087
0.040"	– 0.0168 ± 0.00024	4.91 ± 0.011
0.055"	– 0.0321 ± 0.00069	4.86 ± 0.017
0.030" and 0.040"	– 0.0274 ± 0.00055	4.85 ± 0.015
Unknown	– 0.0213 ± 0.00018	4.67 ± 0.0054

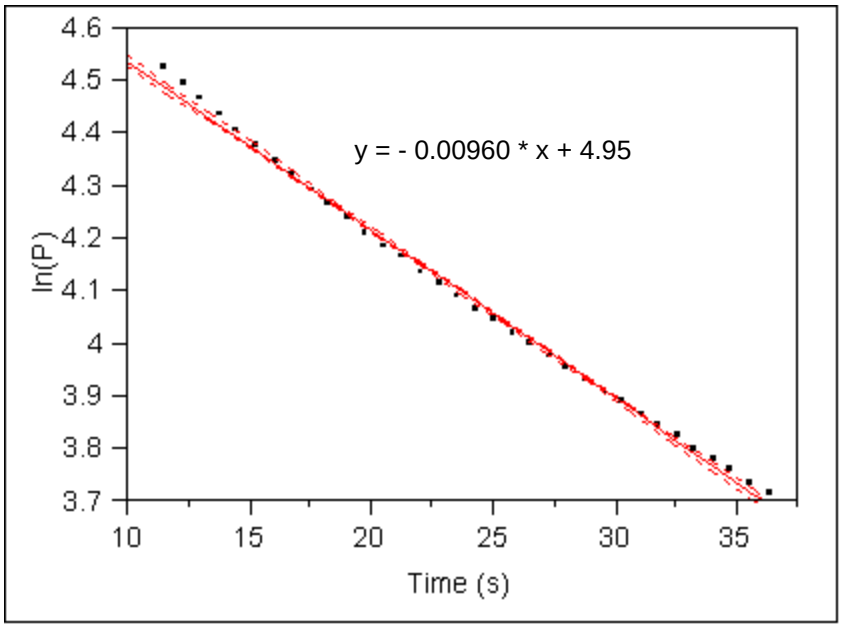

Figure 8. Determination of K' using 0.030" orifice

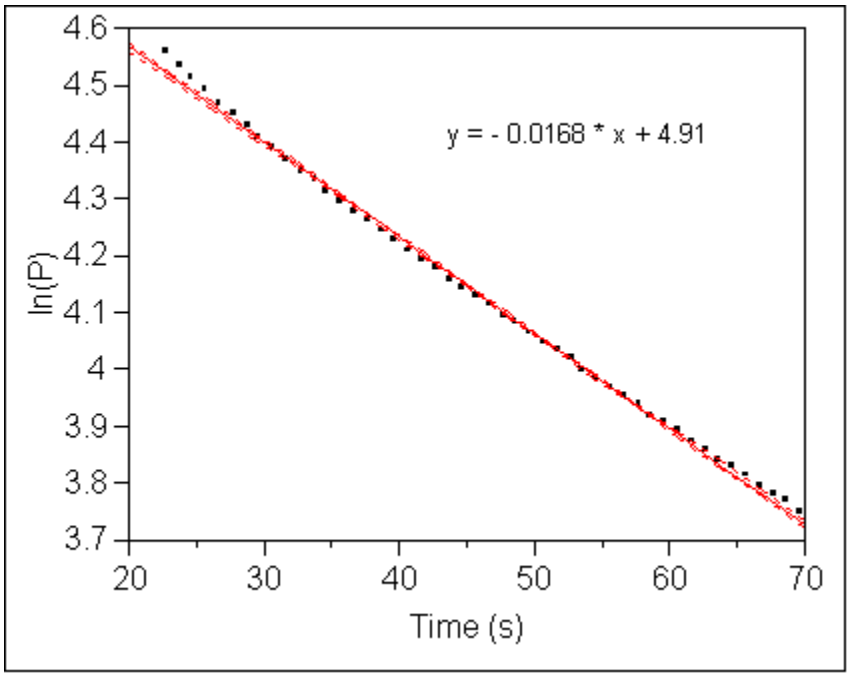

Figure 9. Determination of K' using 0.040" orifice

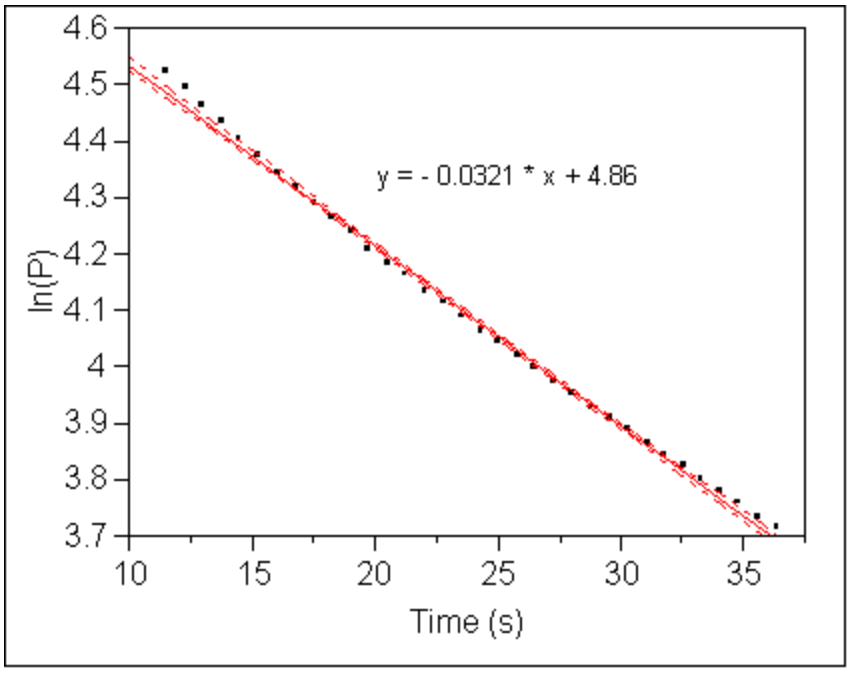

Figure 10. Determination of K' using 0.055" orifice

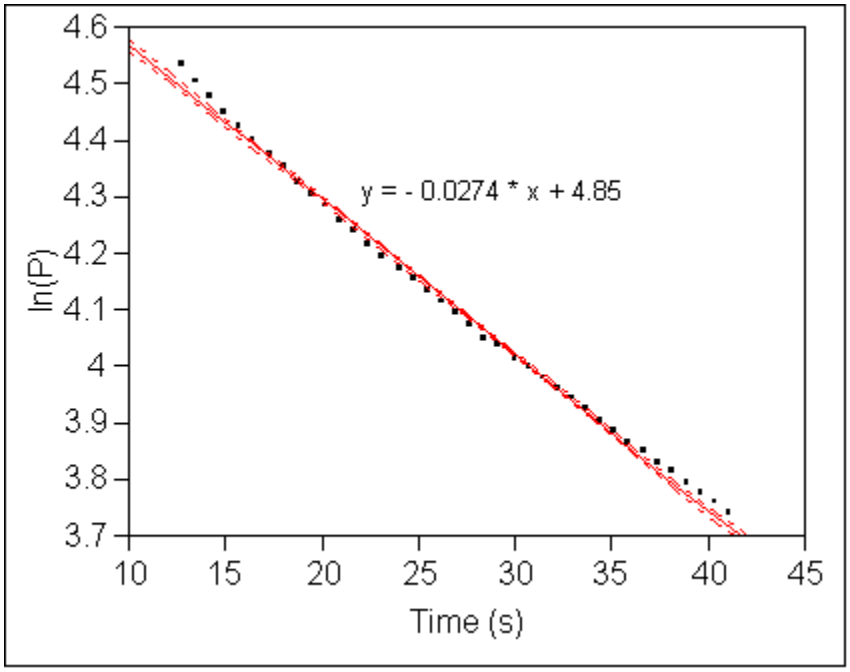

Figure 11. Determination of K' using 0.030" and 0.040" orifices

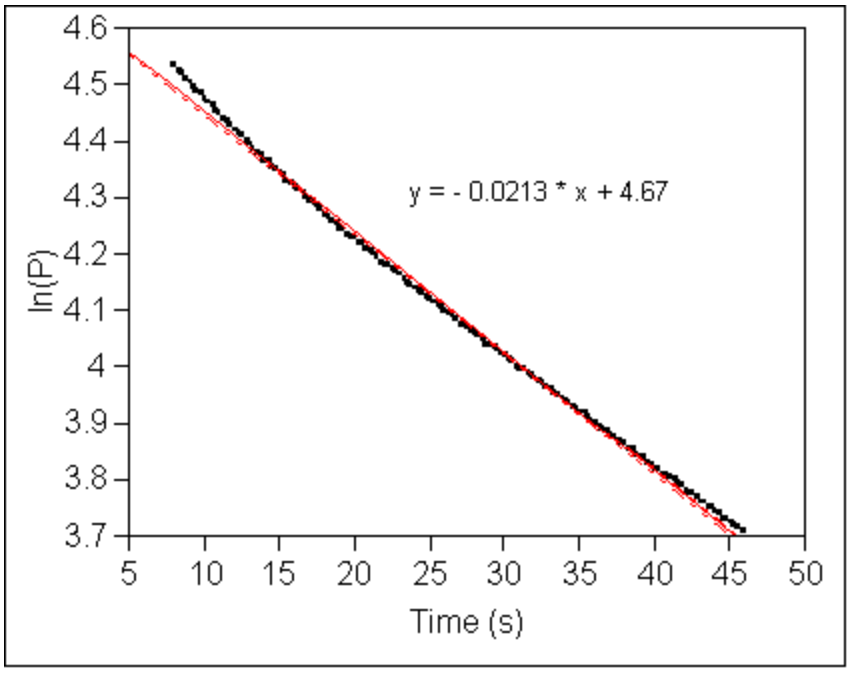

Figure 12. Determination of diameter of unknown orifice

The magnitude of the slope of the plot of ln(P) versus t is proportional to the diameter squared, which is proportional to the area of the orifice (or the sums of the areas of the open orifices). As the total area of the open orifices increases, the magnitude of the slope increases. The slope of the simultaneous discharge of the 0.030" and 0.040" orifices was – 0.0274 while the sum of the slopes for the 0.030" and 0.040" individual orifices was – 0.0264. These values should be equal because the total area of the 0.030" and 0.040" orifices equals the sum of the areas of the 0.030" and 0.040" orifices, but they differ by 3.7%. The slope of the simultaneous discharge of the 0.030" and 0.040" orifices had a smaller magnitude than the sum of the slopes of the 0.030" and 0.055" individual orifices, which was – 0.331. This result is logical because the sum of the areas of the 0.030" and 0.040" orifices is less than the sum of the areas of the 0.030" and 0.055" orifices. The slope of the simultaneous discharge of the 0.030" and 0.040" orifices also had a smaller magnitude than the slope of the 0.055" orifice, which was – 0.321. The total area of the 0.030" and 0.040" orifices (0.00785 in^2) is less than the area of the 0.055" orifice (0.00950 in^2), so the flow rate out of the tank is smaller for the 0.030" and 0.040" orifices than for the 0.55" orifice. Therefore, the tank bleeds faster when the 0.055" orifice is open than when both the 0.030" and 0.040" orifices are open.

The mass in the tank over time for the three orifices with known diameters was compared. The maximum pressure that could be achieved in the tank was about 75 psig, so the experimental data was normalized so the initial pressure at t = 0 was 75 psig. The expression relating the mass in the tank to time was determined using Equation 12, where f is the fraction of mass remaining in the tank, P is the pressure as a function of time, and γ is the specific heat capacity ratio for air. The initial mass in the tank was calculated to be 76.2 g using the ideal gas law. The volume of the tank was given in the lab manual, and the temperature was measured. As Fig. 13 demonstrates, the mass of air in the tank decreases at the fastest rate through the 0.055" orifice and the slowest rate through the

0.030” orifice. The experimental data suggest that as the orifice area increases, the rate of discharge increases.

.

$$P = P_0 f^{\gamma} \tag{12}$$

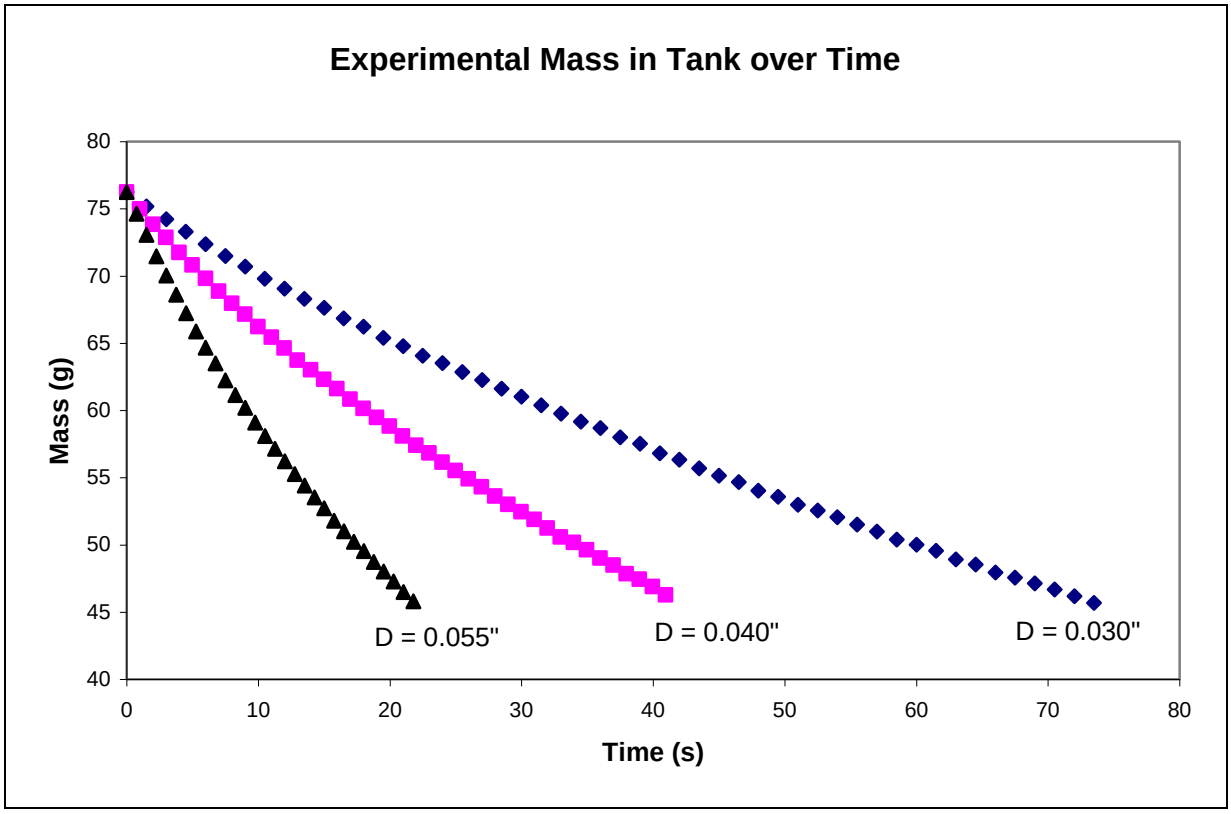

Figure 13. Experimental mass of air in tank over time

A plot comparing the theoretical models for the pressure in the tank versus time for the 0.030”, 0.040”, and 0.055” orifices is shown in Fig. 14. The models were developed using Equation 13, where the experimental K’ values determined from the plots of ln(P) versus time were used. The plots were normalized such that the initial pressure in the tank was 90 psig and the final pressure was 30 psig. The tank reached 30 psig in the fastest time when the 0.055” orifice was open and the slowest time when the 0.030” orifice was open.

$$P = P_0 e^{K' d^2 t} \tag{13}$$

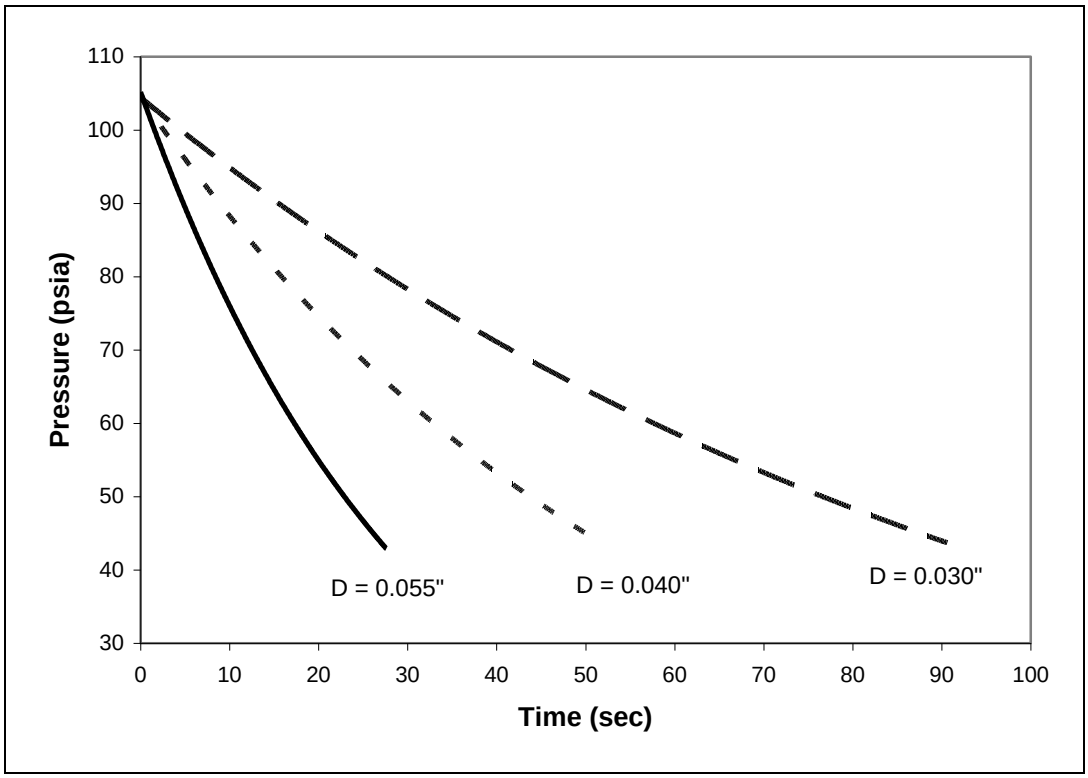

Figure 14. Tank pressure versus time for orifices of different sizes

The theoretical models for the pressure in the tank versus time for each orifice were used to plot the theoretical mass of air remaining in the tank for an initial pressure of 90 psig and a final pressure of 30 psig. Fig. 15 displays the theoretical mass of air remaining in the tank versus time when the air is discharged through each of the three orifices with known diameters. The model for the mass of air in the tank as a function of time was developed by combining Equations 12 and 13 and is shown below in Equation 14. The initial mass of air in the tank assuming an initial pressure of 90 psig was calculated to be 89.0 g using the ideal gas law. The fraction of mass remaining in the tank when the pressure reached 30 psig was calculated to be 0.543. The relative amount of air that escaped during this time was 45.7%. The absolute amount of air that escaped was calculated to be 40.7 g by multiplying the initial mass of air in the tank by the fraction of gas that escaped. Sample calculations are shown in Appendix B. Figs. 14 and 15 show that the final pressure of 30 psig is reached in 30 sec when the 0.055" orifice is used, 50 sec when the 0.040" orifice is used, and 90 sec when the 0.030" orifice is used.

$$m = m_0 e^{\frac{K' d^2 t}{\gamma}} \qquad (14)$$

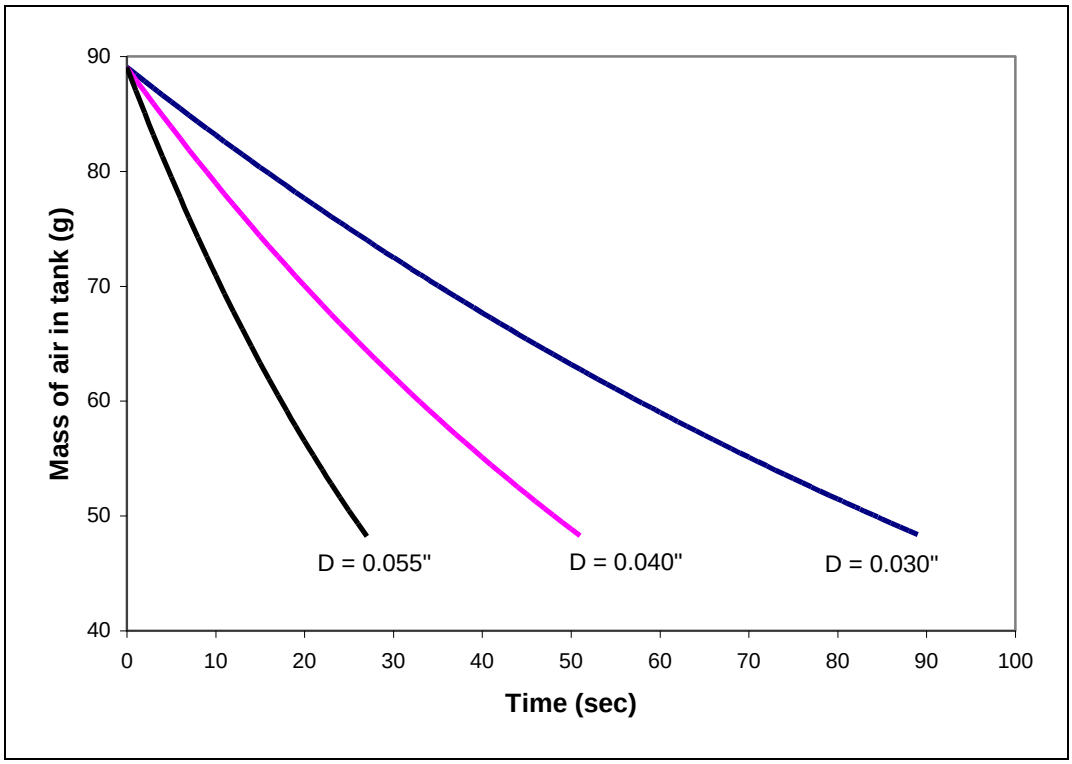

Figure 15. Mass of air in tank versus time for orifices of different sizes

There were several sources of error in each part of this experiment. In the determination of the critical pressure ratio, it is difficult to determine the exact pressure at which the mass flow rate begins to change. Theoretically, the slope of the plot of mass flow rate versus pressure ratio is close to zero near the critical pressure ratio. In other words, the mass flow rate changes gradually in the region close to the critical pressure ratio. Therefore, there is some error in the determination of the downstream pressure at which the mass flow rate begins to change. Since the downstream pressure was increased in increments of 1 – 2 psi in the range near the critical pressure ratio, there was an error of 1 – 2 psi in P2 due to the size of the increments. Also, there were small random errors in the last digits of the digital manometer and flow meter readings.

In the discharge coefficient determination, there were random errors in the last digits of the digital manometer and flow meter readings. Also, there was a random error in the scale markings on the differential manometer. The water level in the manometer fluctuated while measurements were being taken, increasing the error in the measurements. In the tank bleeddown experiment, there was some error in the calibration equation for the Schaevitz strain gauge. There were also errors in the plots of ln(P) versus time. In each plot, the experimental data curved slightly, so the line of best fit did not appear to fit the data well. However, the R^2 values of the plots ranged from 0.9965 to 0.9988, so the experimental data had fairly strong linear correlations. There was also error in the average experimental K' value because each of the calculated K' values was different.

Conclusions/Recommendations

In summary, both the critical flow and subsonic flow of a compressible gas through a nozzle and several orifices were studied in this lab. The critical pressure ratio for a critical flow nozzle was calculated to be 0.704. The inverse of r_c, which is the minimum ratio of inlet pressure to exit pressure for sonic flow, was 1.42. This value is greater than the manufacturer's claim of 1.2, so the experimental data contradicts the data provided by the manufacturer (Willson, 2008).

The calibration equation for the nozzle performance curve was determined to be y = 1.012 x – 0.001166, where y is the flow rate determined from the performance curve in lb / min and x is the flow rate from the NIST-calibrated digital flow meter in lb / min. The calibration plot had small confidence intervals for the slope and intercept, so it was very precise. The plot of the difference between the performance curve flow rate and the true flow rate illustrates that the performance curve is most accurate in the region near 0.0972 lb / min. The experimental procedure could be improved by including several types of flow meters so that the performance curve could be compared to other methods of flow measurement.

In addition, the discharge coefficients and Reynolds numbers of subsonic flow through an orifice were calculated for three different pressure drops. The experimental discharge coefficients were calculated to be 0.920 at a Reynolds number of 12700, 0.926 at a Reynolds number of 18500, and 0.935 at a Reynolds number of 21600. These values were about 47% larger than the literature values of the discharge coefficients. The discrepancies are most likely due to errors in the pressure drop readings. The relative error could be decreased by using a more precise manometer (one with more markings and smaller gradations) or by increasing the magnitudes of the pressure drops studied (Willson, 2008).

Finally, a tank was filled with air at a high pressure and then discharged through various orifices as its pressure was monitored versus time. The slopes of plots of ln(P) versus t and the diameters of the open orifices were used to determine the orifice constant K'. The average value of K' was -10.67 ± 0.31. This value and the slope of the unknown orifice plot were used to find the diameter of the unknown orifice, which was calculated to be 0.045". Assuming the tank was initially filled with an air pressure of 90 psig and discharged until the final pressure reached 30 psig, 40.7g of air (or 45.7% of the initial mass in the tank) escaped from the tank. The slope of the simultaneous discharge through the 0.030" and 0.040" orifices is less than the slope of the discharge through the 0.055" orifice because the area of the 0.055" orifice is larger than the sum of the areas of the 0.030" and 0.040" orifices (Willson, 2008).

Appendix A

Experimental Data

Atmospheric Temperature: 73.5 F
Atmospheric Pressure: 29.4 in Hg

Table A-1. Critical pressure ratio determination for P1 = 90 psig

Trial	P1 (psig)	P2 (psig)	Q (STD L/min)
1	88.4	2.6	91.0
2	87.8	7.6	90.7
3	87.2	12.6	90.6
4	86.9	17.6	90.6
5	86.7	22.6	90.5
6	86.4	27.6	90.2
7	86.3	32.6	90.4
8	86.3	37.6	90.4
9	86.1	42.6	90.4
10	85.8	47.7	90.4
11	85.7	52.6	90.3
12	85.6	57.5	88.9
13	85.4	62.7	85.4
14	86.1	67.5	80.2
15	84.9	72.5	72.9
16	84.8	77.6	62.3
17	84.8	82.6	46.4
18	83.7	49.8	90.0
19	83.6	51.0	89.8
20	83.5	51.9	89.6
21	83.4	53.2	89.5
22	83.4	54.2	89.4
23	83.2	55.2	89.2
24	83.3	56.0	88.9
25	83.0	57.1	88.1
26	83.0	58.0	87.8
27	82.7	58.8	87.3

Table A-2. Critical pressure ratio determination for P1 = 70 psig

Trial	P1 (psig)	P2 (psig)	Q (STD L/min)
1	69.2	2.0	76.9
2	68.7	12.1	76.7
3	68.6	22.1	76.7
4	68.5	31.9	76.6
5	68.4	42.2	76.4
6	68.5	52.0	72.6
7	68.2	47.2	75.0
8	68.0	45.2	75.6
9	68.0	43.1	76.0
10	68.8	57.5	67.5
11	69.5	64.2	57.2

Table A-3. Critical pressure ratio determination for P1 = 50 psig

Trial	P1 (psig)	P2 (psig)	Q (STD L/min)
1	50.5	1.3	60.4
2	50.5	11.7	60.3
3	50.5	21.2	60.3
4	50.5	34.7	59.0
5	50.3	28.3	60.3
6	50.4	30.4	60.2
7	50.4	32.1	59.8
8	50.5	33.1	59.6
9	50.8	39.5	55.8
10	51.4	45.5	48.9

Table A-4. Critical pressure ratio determination for P1 = 30 psig

Trial	P1 (psig)	P2 (psig)	Q (STD L/min)
1	30.3	0.6	41.2
2	30.0	13.6	41.1
3	30.3	21.2	39.0
4	30.3	16.6	41.1
5	30.1	17.7	40.7
6	30.0	10.5	41.2
7	30.0	11.3	41.2
8	30.0	12.2	41.1
9	34.4	37.6	0.0
10	30.1	26.9	30.8
11	30.7	29.0	27.2

Table A-5. Discharge coefficient data

ΔP (in H2O)	P1 (psig)	T1 (F)	Q (STD L/min)
5.1	27.7	73.4	39
11.0	46	73.8	56.8
15.0	55.8	73.9	66.3

Table A-6. Strain gauge transducer calibration

Manometer Pressure (psig)	Transducer Voltage (mV)
20	5.04
31.6	7.95
41.9	10.5
50.6	12.7
61	15.3
70.8	17.6
80.6	20.05
84.4	21

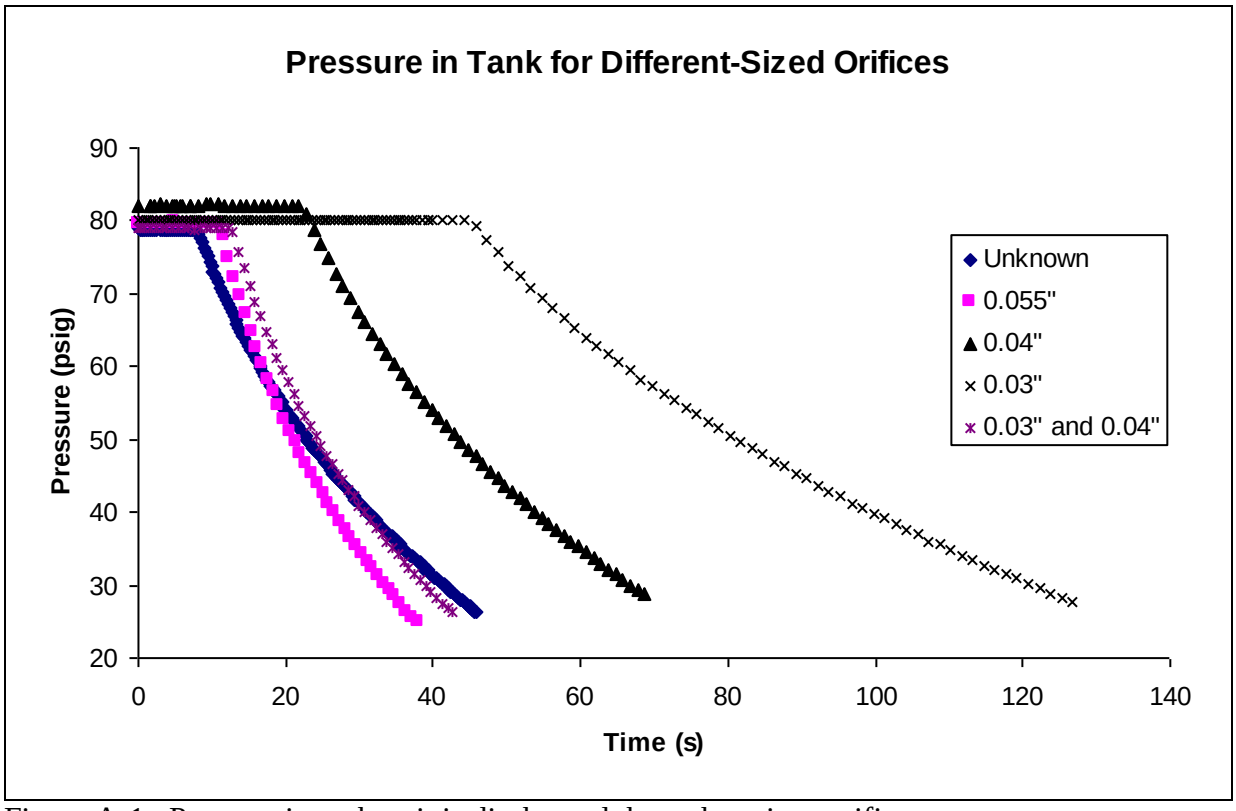

Figure A-1. Pressure in tank as it is discharged through various orifices

Appendix B

Sample Calculations

Critical Pressure Ratio Determination

Calculation of critical pressure ratio using $P1 \approx 90$ psig as example:

$$r_c = \frac{P_2}{P_1} = \frac{(83.4 + 14.4)}{(51.9 + 14.4)} = 0.677 \qquad \text{(B-1)}$$

Where r_c = critical pressure ratio
P_1 = absolute pressure upstream of nozzle (psia)
P_2 = absolute pressure downstream of nozzle (psia)

Calculation of critical mass flow rate from the critical flow nozzle performance plot using $P1 \approx 90$ psig as example:

$$w_{CFN} = \frac{KP_1}{\sqrt{T_1}} = \frac{0.05496 * 97.8}{\sqrt{533.6}} = 0.233 \qquad \text{(B-2)}$$

Where w = mass flow rate (lb / min)
K = a weak function of pressure (obtained from plot in lab manual)
P = absolute inlet pressure (psia)
T = absolute inlet temperature (R)

Calculation of critical mass flow rate from the NIST digital flow meter using $P1 \approx 90$ psig as example:

$$w = Q_{DFM} \bullet \rho_{DFM} = \frac{Q_{DFM} P_{atm} M_{air}}{RT_{atm}} = \frac{1.49 * 0.980 * 29}{0.08206 * 296.4} * \left(\frac{1\ lb}{454\ g} \right) * \left(\frac{60\ s}{1\ \text{min}} \right) = 0.231 \qquad \text{(B-3)}$$

Where w = mass flow rate (lb / min)
Q = volumetric flow rate (L/s)
ρ = density (g/L)
P = atmospheric pressure (atm)
T = atmospheric temperature (K)
M = molecular weight of air (g / mol)
R = ideal gas constant (L atm / mol K)

Q was converted from standard to actual using the equation shown in the discharge coefficient sample calculations section. The line of best fit for w_{dfm} vs. w_{cfn} was determined using the linear regression equations shown in the tank bleeddown sample calculations section.

Discharge Coefficient Determination

All sample calculations shown are for ΔP = 5.1 in H2O.

Calculation of actual volumetric flow rate from standard volumetric flow rate:

$$Q_{actual} = Q_{standard}\left(\frac{P_{standard}}{P_{actual}}\right)\left(\frac{T_{actual}}{T_{standard}}\right) = 39.0\left(\frac{14.7}{14.4}\right)\left(\frac{533.5}{492}\right) = 43.2 \qquad \text{(B-4)}$$

Where Q = volumetric flow rate (L / min)
P = absolute pressure (psia)
T = absolute temperature (R)

Calculation of Reynolds number of flow through orifice:

$$V = \frac{Q}{A} = \frac{4Q}{\pi d^2} = \frac{4 * 719.5}{\pi * (0.4648)^2} = 4240 \qquad \text{(B-5)}$$

$$\rho_{atm} = \frac{P_{atm} M_{air}}{RT_{atm}} = \frac{0.980 * 29}{82.06 * 296.4} = 0.001168 \qquad \text{(B-6)}$$

$$\text{Re} = \frac{\rho_{atm} V_{or} d_{or}}{\mu_{air}} = \frac{0.001168 * 4240 * 0.4648}{1.81 * 10^{-4}} = 12720 \qquad \text{(B-7)}$$

Where Re = Reynolds number (unitless)
Q = actual volumetric flow rate through orifice (mL / sec)
V = velocity through orifice (cm / sec)
ρ = density of air at atmospheric conditions (g / mL)
μ = viscosity of air (g / cm s)
d = diameter of orifice (cm)
A = area of orifice (cm^2)

Calculation of density of air upstream of orifice:

$$\rho_1 = \frac{P_1 M_{air}}{RT_1} \approx \frac{(P_{atm} + \Delta P) M_{air}}{RT_{atm}} = \frac{(0.980 + 0.013) * 29}{82.06 * 296.4} = 0.001184 \qquad \text{(B-8)}$$

Where ρ = density of air at orifice (g / mL)
P = absolute pressure (atm)
ΔP = pressure drop across orifice (atm)
T = atmospheric temperature (K)
M = molecular weight of air (g / mol)
R = ideal gas constant (mL atm / mol K)

Calculation of Y for $\beta < 0.25$:

$$Y = \sqrt{r^{2/\gamma}\left(\frac{\gamma}{\gamma-1}\right)\left(\frac{1-r^{(\gamma-1)/\gamma}}{1-r}\right)} = \sqrt{0.987^{2/1.4}\left(\frac{1.4}{1.4-1}\right)\left(\frac{1-0.987^{(1.4-1)/1.4}}{1-0.987}\right)} = 0.993 \quad \text{(B-9)}$$

Where Y = expansion factor
$r = P_2 / P_1 = P_{atm} / (P_{atm} + \Delta P)$
$\gamma = c_p / c_v$ = specific heat capacity ratio = 1.4 for air

Calculation of discharge coefficient of orifice:

$$Q = C_d A_2 Y \sqrt{\frac{2g_c(\Delta P)}{\rho_1(1-\beta^4)}} \quad \text{(B-10)}$$

$$C_d = \frac{Q}{A_2 Y}\sqrt{\frac{\rho_1(1-\beta^4)}{2g_c(\Delta P)}} = \frac{719.5}{0.1697 * 0.993}\sqrt{\frac{0.001184(1-0.244^4)}{2(1)(12704)}} = 0.920$$

Where Q = volumetric flow rate (mL / sec)
C_d = discharge coefficient
A_2 = area of orifice = $\pi d^2/4$ (cm^2)
Y = expansion factor
$\beta = d_2 / d_1$ = ratio of orifice diameter to pipe diameter
ρ = density of air at orifice (g / mL)
ΔP = pressure drop across orifice (dyne / cm^2)

Tank Bleeddown Calculations

Linear regression and confidence limit calculations for the equation $y = a + bx$ using the plot of ln(P) versus time for the 0.030" orifice as an example:

$$b = \frac{\Sigma xy - \frac{(\Sigma x)(\Sigma y)}{N}}{\Sigma x^2 - \frac{(\Sigma x)^2}{N}} \quad \text{(B-11)}$$

$$b = \frac{(45.7 * 4.54 + 47.2 * 4.52 + 48.73 * 4.50 + \ldots) - \frac{(45.7 + 47.2 + 48.7 + \ldots)(4.54 + 4.52 + 4.50 + \ldots)}{4}}{(45.7^2 + 47.2^2 + 48.7^2 + \ldots) - \frac{(45.7 + 47.2 + 48.7 + \ldots)^2}{4}}$$

$$b = -0.00960$$

$$a = \bar{y} - b\bar{x} = 4.16 + 0.00960 * 82.5 = 4.95 \quad \text{(B-12)}$$

$$s_{y/x} = \sqrt{\frac{\Sigma(yi - \hat{y}i)^2}{N-2}} \tag{B-13}$$

$$s_{y/x} = \sqrt{\frac{(4.54-4.51)^2 + (4.52-4.50)^2 + (4.50-4.48)^2 + \ldots}{50-2}} = 7.93*10^{-3}$$

$$s_a = s_{y/x}\sqrt{\frac{\Sigma xi^2}{N\,\Sigma(xi-\bar{x})^2}} \tag{B-14}$$

$$s_a = 7.93*10^{-3}\sqrt{\frac{45.7^2 + 47.2^2 + 48.7^2 + \ldots}{50*[(45.7-82.5)^2 + (47.2-82.5)^2 + (48.7-82.5)^2 + \ldots]}} = 0.00442$$

$$s_b = \frac{s_{y/x}}{\sqrt{\Sigma(xi-\bar{x})^2}} \tag{B-15}$$

$$s_b = \frac{7.93*10^{-3}}{\sqrt{(45.7-82.5)^2 + (47.2-82.5)^2 + (48.7-82.5)^2 + \ldots}} = 5.18*10^{-5}$$

$$\alpha = a \pm t_{n-2}s_a = 4.95 \pm 1.96*0.00442 = 4.95 \pm 0.0087 \tag{B-16}$$

$$\beta = b \pm t_{n-2}s_b = -0.00960 \pm 1.96*5.18*10^{-5} = 0.00960 \pm 0.00010 \tag{B-17}$$

Where
- a = intercept
- b = slope
- x = time (sec)
- y = ln[P (psia)]
- N = number of data points = 50
- $\bar{x}$ = average x-value (sec)
- $\bar{y}$ = average y-value
- t_{n-2} = Student's t-value for 95% confidence, 48 degrees of freedom = 1.96
- α = 95% confidence limits for intercept
- β = 95% confidence limits for slope

Calculation of K' using 3" orifice as example:

$$\ln P = K' d^2 t + constant \quad \text{(B-18)}$$

$$K' = \frac{m}{d^2} = \frac{-0.00960}{0.030^2} = -10.67 \quad \text{(B-19)}$$

Where P = absolute pressure (psia)
d = diameter of orifice (in)
t = time (sec)
K' = function of temperature, molecular weight, and volume (constant in this experiment)
m = slope

Calculation of 95% confidence interval for K':

$$CI = K' \pm t_{n-1} s / \sqrt{n} = -10.7 \pm 3.182 * 0.196 / \sqrt{4} = -10.67 \pm 0.31 \quad \text{(B-20)}$$

Where K' = function of temperature, molecular weight, and volume
n = number of data points = 4
t_{n-1} = Student's t-value for n = 4, $\alpha = 0.025$
s = standard deviation of K'

Calculation of unknown orifice diameter:

$$d = \sqrt{\frac{m}{K'}} = \sqrt{\frac{-0.0213}{-10.67}} = 0.045 \quad \text{(B-21)}$$

Where d = diameter of orifice (in)
K' = function of temperature, molecular weight, and volume (constant in this experiment)
m = slope

Calculation of initial mass of air in tank for P0 = 90 psig:

$$PV = nRT = \frac{m}{M} RT \quad \text{(B-22)}$$

$$m = \frac{PVM}{RT} = \frac{7.25 * 10.3 * 29}{0.08206 * 296.4} = 89.04\ g$$

Where m = mass of air in tank (g)
P = absolute pressure (atm)
T = atmospheric temperature (K)
M = molecular weight of air (g / mol)
R = ideal gas constant (L atm / mol K)

Calculation of mass fraction of air remaining in tank:

$$P = P_0 f^{\gamma} \tag{B-23}$$

$$f = \left(\frac{P}{P_0}\right)^{1/\gamma} = \left(\frac{44.4}{104.4}\right)^{1/1.4} = 0.543$$

Where P = absolute pressure (psia)
P_0 = absolute initial pressure (psia)
$f = m / m_0$ = mass fraction of fluid remaining in tank
$\gamma = c_p / c_v$ = specific heat capacity ratio = 1.4 for air

Appendix C

Safety Considerations

The experimenters wore long pants, closed-toed shoes, and safety glasses in the lab. No harmful chemicals were handled during this experiment. Air under high pressure was a safety concern in this lab. The experimenters were careful when turning valves and opening orifices.

Appendix D

Experimental Apparatus

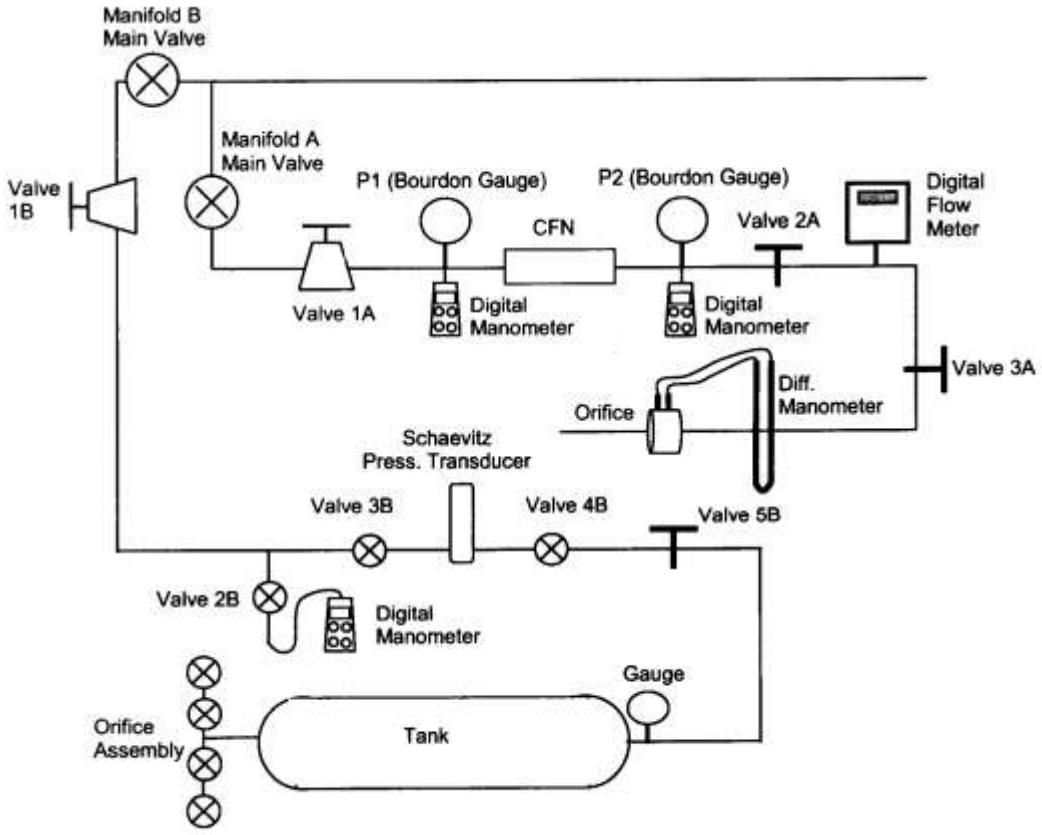

Figure D-1. Setup of experimental apparatus (Willson, 2008)

References

Willson, C. Grant. (2008). *Compressible Gas Flow*. Lab Handout ChE 253M, The University of Texas at Austin.

Green, D. W., & Perry, R. H. (Eds.). (2008). *Perry's Chemical Engineers' Handbook* (8th ed.). New York: McGraw-Hill.